



Characterization of the floral traits, pollen micromorphology and DNA barcoding of the edible flowers from three basil taxa (Lamiaceae)

Miriam Bazzicalupo · Federica Betuzzi · Jessica Frigerio · Werther Guidi Nissim · Fabio Rapallo · Barbara Ruffoni · Laura Cornara · Andrea Copetta

Received: 12 February 2024 / Accepted: 1 September 2024
© The Author(s) 2024

Abstract The edible flowers sector is expanding due to the popularity and uses in culinary recipes of different species. In particular, flowers of *Ocimum basilicum* L. and related taxa are increasingly used for their aromas and nutritional value. However, there is limited information regarding their morphological characteristics and molecular profiles, which are both important to perform a quality control of food,

and to avoid contaminations. Hence, our aim was the study of three basil taxa (*O. basilicum* ‘Cinnamon’, *O. basilicum* ‘Blue Spice’, and the hybrid *O. × africanum* Lour.) to obtain data useful for taxa identification and to understand which traits could be linked to their chemodiversity. The plants were grown in a greenhouse starting from seeds. Flowers were collected at anthesis; the morphology of calyxes, corolla and pollen grains was characterized; DNA barcoding analyses were performed. All taxa were identified only as *O. basilicum* by molecular analyses, but two haplotypes were distinguishable. All taxa were identifiable due to the presence/absence of specific glandular trichomes, and by pollen size and number of colpi. ‘Cinnamon’ and *O. × africanum* showed more morphological affinities to each other, but histochemical analyses suggested the separation of the three taxa. Pollen grains from ‘Cinnamon’ had the smallest diameter in polar view and were hexacolpate, while ‘Blue Spice’ pollen showed the highest diameter with grains being hexacolpate/octacolpate, similarly to *O. × africanum*. Our interdisciplinary study provides the first information for authenticating these basil cultivars in packaged products for human consumption.

Supplementary Information The online version contains supplementary material available at <https://doi.org/10.1007/s10722-024-02170-5>.

M. Bazzicalupo · F. Betuzzi · L. Cornara
Department of Earth, Environment and Life Sciences,
University of Genova, Corso Europa 26, 16132 Genoa,
Italy

M. Bazzicalupo
Jodrell Laboratory, Royal Botanic Gardens,
Kew, Richmond, Surrey TW9 3DS, UK

J. Frigerio (✉) · W. G. Nissim
Department of Biotechnology and Biosciences, University
of Milano-Bicocca, Piazza Della Scienza 2, 20126 Milan,
Italy
e-mail: jessica.frigerio@unimib.it

F. Rapallo
Department of Economics (DIEC), University of Genova,
Via F. Vivaldi, 5, 16126 Genoa, Italy

B. Ruffoni · A. Copetta
Research Centre for Vegetable and Ornamental Crops,
Council for Agricultural Research and Economics, CREA-
OF, 18038 Sanremo, Italy

Keywords *Ocimum basilicum* · Glandular trichomes · Edible flowers · Taxon identification · Floral traits · DNA sequencing

Introduction

In recent years, the consumption of edible flowers for human nutrition has increased considerably worldwide (Fernandes et al. 2018; Pires et al. 2018; Najar et al. 2019). Traditionally, edible flowers were mainly used as hot beverages and tisanes for self-care and to aid in healing from various forms of sickness. However, nowadays, they are incorporated into various recipes, including salads, pies, and desserts, often serving as garnish to add color and enhance the aesthetic appeal of meals (Mlcek and Rop 2011; Husti et al. 2013).

Among the edible plant taxa with very tasty flowers are basil: they are sweet due to the presence of drops of nectar, while the aromatic notes vary depending on the cultivars and hybrids. One of the most famous, *Ocimum basilicum* L. (sweet basil), is a medicinal herb of economic importance. Its leaves are widely used for dried and fresh culinary recipes as flavorings in foods and drinks (Dudai et al. 2020).

Many basil cultivars are cultivated to harvest the leaves, which are used to make the “pesto” sauce (‘Genovese’ or ‘Italiko’) (Laura et al. 2023), while others are grown for ornamental purposes (Makri and Kintzios 2008; Švecová and Neugebauerová 2010). Recently, basil cultivars of variable size, growth habit, color, and aromas (including lemon, anise, liquorice, cinnamon, and others) are becoming increasingly popular for culinary purposes (Simon et al. 1999), and those used as edible flowers are not an exception.

Basil’s aroma is determined by several volatile aromatic compounds released by flowers and leaves: the composition, concentration, and ratios of these aromatic compounds influence the sensory features. The secondary compounds (such as terpenes and phenylpropanoids) that constitute essential oils (EOs) are synthesized and stored in the glandular trichomes (mainly capitate and peltate trichomes) present on the epidermis of basil leaves and flowers (Gang et al. 2001; Maurya et al. 2019). The EOs of *O. basilicum* have essential biological activities (response to environmental stimuli, defence against herbivores and pathogenic microorganisms, attraction for pollinators, communication between plants), and their variation in composition depend on the agronomic conditions, the age of the plant, and chemotypes (Copetta et al. 2006; Beatovic et al. 2015).

The presence of specific secondary compounds was found to be indicative of a particular taste: for example, the presence of linalool imparts a sweet/floral taste; eucalyptol is responsible for the fresh/eucalyptus-like aroma; eugenol tastes like clove; methyl chavicol resembles the anise aroma; methyl cinnamate is responsible for the cinnamon flavour; citral, neral, and geranial are linked to a citrus aroma (Brechbill 2007; Fischer et al. 2011; Patel et al. 2021). The ratios of these and other volatile compounds define the chemotype. Recently, the flower volatile profiles of three ornamental sweet basil cultivars with exciting tastes, namely *O. ×africanum* Lour. (lemon peel taste), *O. basilicum* ‘Cinnamon’ (cinnamon taste), and *O. basilicum* ‘Blue Spice’ (spicy taste), were analyzed. The results indicated the possibility to distinguish each cultivar based on the specific chemotype. Geranial/neral (citrus aroma), linalool/methyl cinnamate (floral/cinnamon aroma), and bisabolene/β-ocimene (warm spicy balsamic/warm herbaceous aroma) were characteristic of *O. ×africanum*, ‘Cinnamon’, and ‘Blue Spice’, respectively (Marchioni et al. 2020a). *Ocimum ×africanum* (synonym of *O. ×citriodorum* according to www.powo.science.kew.org, accessed by 8 February 2024), popularly known as lemon basil, is grown as a culinary herb in Mediterranean and Asian countries, and often used in both Asian and Mediterranean cuisines to add the scent and flavour of lemon to dishes (Majdi et al. 2020). This plant could be used as a substitute for lemon grass or other lemon scented culinary species (Al-Kateb and Mottram 2014). Furthermore, the economic interest in this hybrid is increasing as it is exploited by chemical, pharmaceutical and food industries to produce condiments, oral hygiene products, perfumes and ice cream (Paulus et al. 2019). *Ocimum basilicum* ‘Cinnamon’ (also called Mexican spice basil) is often used to prepare baked products, teas, fruit salads, vinegars and jellies due to the spicy flavour of its leaves and flowers. It can be considered as an alternative to powdered cinnamon. In addition, the dried herb is added to potpourri while the essential oil represents an excellent ingredient in perfumery to create perfumes (Wesolowska and Jadczyk 2016). *Ocimum basilicum* ‘Blue Spice’ is used as a flavouring agent in savory dishes and for the extraction of its essential oils which have shown strong antioxidant properties (Beatovic et al. 2015).

While data on the distribution and types of trichomes responsible for the production of essential oils in basil leaves are available in the literature (Werker 1993; Gang et al. 2001), information regarding the trichomes present in their edible flowers is very scarce. The distribution and the types of glandular and non-glandular trichomes have great taxonomic value and have been widely used for understanding systematic and phylogenetic relationships in Lamiaceae (Werker et al. 1985a, b; Cantino 1990; Maleci Bini and Servettaz 1991; Karousou et al. 1992); this kind of data is also employed to delimit taxa at the infra-section (Bhattacharjee 1980, 1982; Navarro and El Oualidi 2000) and for the identification of cultivars or ecotypes (Zhang et al. 2023).

The recent increased consumption of edible flowers has led to a more complex production chain and the delivery of packaged commercial compositions (Marchioni et al. 2020b), which are often set up with multiple species. The consumption of certain Lamiaceae taxa is considered safer, as they generally exhibit no allergenicity and possess anti-allergic activities (Sim et al. 2019). However, to overcome the problem of mystification and misidentification, it is necessary to deepen the micromorphological analysis and molecular tools of these edible taxa to authenticate plant products and ensure food safety (Cornara et al. 2018; Frigerio et al. 2021). In fact, in cases of fraud or adulteration, the plant material declared in the preparations is not always actually present, but is replaced with other species, even toxic or of lesser value (Nithaniyal et al. 2017; Cornara et al. 2018; Grazina et al. 2020). To discriminate closely related taxa, pollen characteristics can also be used (Gul et al. 2019; Bano et al. 2020; Ali et al. 2021; Pospiech et al. 2021; Nabila et al. 2022) and can contribute to the authentication of plant products (Smillie and Khan 2010; Tungmunnithum et al. 2020; Bahadur et al. 2022). Morphological characteristics of *O. basilicum* pollen have been studied by several authors (Harley et al. 1992; Arogundade and Adedeji 2010; Doaigey et al. 2018; Azzazy 2019; Gul et al. 2019; Bahadur et al. 2022; Kumari et al. 2022), however not all basil taxa have been investigated in terms of pollen micromorphology.

Among the tools used for taxa identification, the DNA barcoding approach is gaining more and more importance as a reliable molecular method, and it is now widely used as a tool to disentangle

the provenance of food products (Galimberti et al. 2015; Mohammed et al. 2017; Frigerio et al. 2019). This approach relies on using short and standardized DNA sequences to distinguish between various taxa. In the case of plants, the commonly analysed DNA sequences are chloroplast DNA (cpDNA) and the internal transcribed spacer (ITS) (Kress et al. 2007; Yao et al. 2010). Through the comparison of barcode sequences derived from unidentified samples with reference databases like NCBI (<https://www.ncbi.nlm.nih.gov>) and BOLD (<https://www.boldsystems.org/>), DNA barcoding allows to recognize species within foods.

Considering the interest in the commercialization of *O. ×africanum*, *O. basilicum* ‘Cinnamon’ and *O. basilicum* ‘Blue Spice’, the lack of morphological and histochemical data about their floral tissues and pollen grains, and the importance of the DNA sequencing approach in the identification of food products, the aims of our work were to: (a) investigate the morphological and molecular differences between the flowers of the three basil taxa to define which traits could be used as a reference for the identification and b) understand which traits could have an impact on their chemo-diversity.

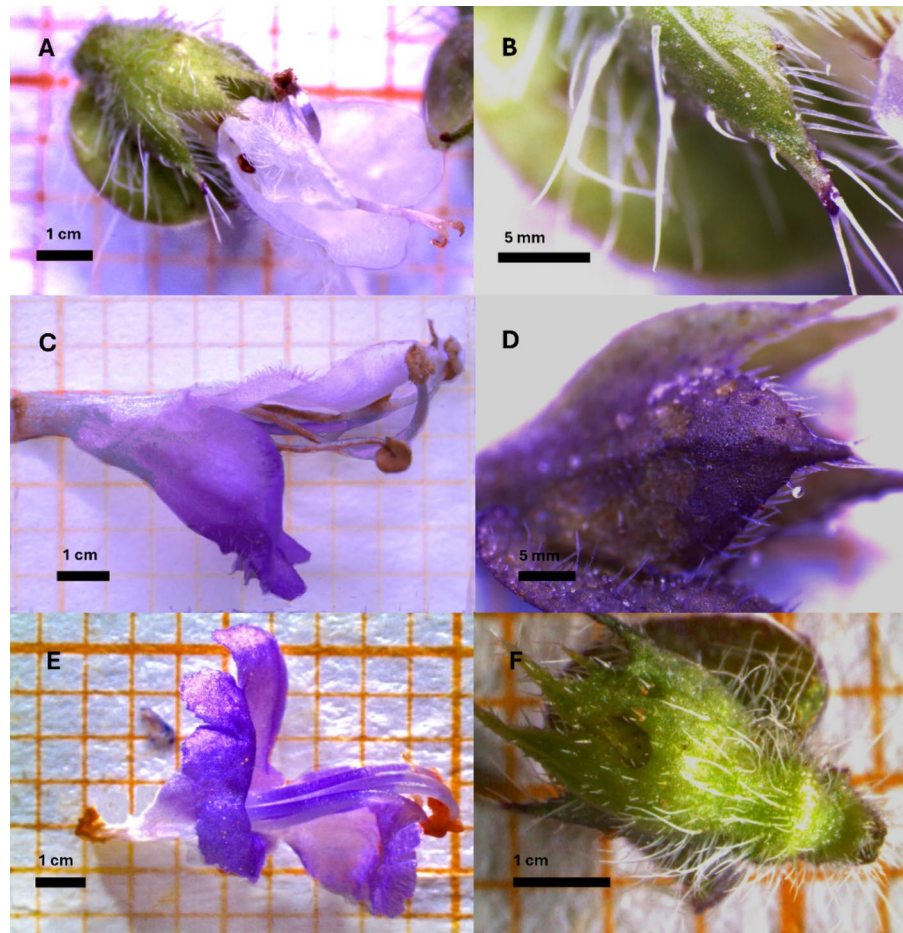
Material and Methods

Plant material and flower production

For all analyses performed in this work, we used full-bloom flowers (Fig. 1) obtained from cultivated plants. Here follow details on the cultivation of the three basil taxa.

The seeds of *O. ×africanum*, *O. basilicum* ‘Cinnamon’ and *Ocimum basilicum* ‘Blue Spice’ were obtained from the Conservatoire National des Plantes à Parfum, Médicinales et Aromatiques (Milly-la-Forêt, France). Basil seeds were sown in alveolus containers (60 holes) filled with peat: sand 2:1. Once reached the stage of development of four true leaves, the plants were transplanted into plastic pots (14-cm diameter) filled with 500 mL of peat and pumice substrate (Hochmoor—Terflor, Capriolo, BS, Italy) with slow-release NPK 14-16-18 fertilizer (Nitrophoska, Eurochem Agro, Cesano Maderno, MB, Italy). The basil plants were cultured in a greenhouse equipped with an anti-insect net at the Research Centre for

Fig. 1 Corolla and calyces of the three *Ocimum* taxa. **A:** *O. ×africanum*; **B:** *O. basilicum* ‘Cinnamon’; **C:** *O. basilicum* ‘Blue Spice’; **D:** *O. ×africanum*; **E:** *O. basilicum* ‘Cinnamon’; **F:** *O. basilicum* ‘Blue Spice’. Bar = 1 cm



Vegetable and Ornamental Crops (CREA, Sanremo, Imperia, Italy; GPS: 43.816887, 7.758900) and watered three times a week. The cultivation method followed the organic system, meaning no pesticides were used: antagonistic insects such as *Aphidius colemani* (parasite), *Chrysoperla carnea*, *Adalia bipunctata*, *Phytoseiulus persimilis* and *Amblyseius swirskii* (predators) (Koppert Italia Srl., Bussolengo, Verona, Italy) were released into the greenhouse and spores of *Bacillus thuringiensis* subsp. *Kurstaki* (Serbios Srl, Badia Polesine, Rovigo, Italy) was sprayed to control the development of caterpillars.

Morphological and data analyses

Morphological data were recorded in 2019 and 2020 on 15 different flowers for each taxon and blooming season; micro-morphological analyses on pollen grains were also performed. Macro- and

micromorphological features of basil flowers were investigated by means of Light and Scanning Electron Microscopy (LM and SEM).

For LM analysis, portions of epidermal peels or sections of fresh calyx and corolla were immediately examined after mounting in distilled water by transmitted light or epifluorescence with a Leica DM 2000 microscope. To detect autofluorescence of polyphenols, flavonoids and other compounds, tissues were then inspected under UV filter (340–380 nm) following Talamond et al. (2015). Fluorol Yellow 088 was used to discern the presence of terpenoids/lipids (Brundrett et al. 1991): in this case, tissues were mounted in 50% glycerol, and observation was carried out under the UV light. In addition, the following histochemical reactions were carried out: Toluidine Blue O (TBO) at pH 4.4 for detecting polyphenols and tannins, Sudan III for total lipids, and Ruthenium Red for non-cellulosic mucopolysaccharides.

For LM analysis of basil pollen, grains were stained directly on a glass slide with a few drops of a basic fuchsin dye dissolved in a glycerin jelly (Lanzoni s.r.l., Bologna, Italy), according to Kraus et al. (1998). Afterward, data were collected on 30 different grains for each taxon, measuring the diameter in polar view (D-PV) and the length of the two axes in equatorial vision. The ratio between the two axes (P/E) was also calculated.

For the analysis of flower samples by scanning electron microscopy, the FineFIX working solution (Milestone s.r.l., Bergamo, Italy) added with 70% ethanol was used overnight at 4 °C, following Chieco et al. (2013). Specimens were then dehydrated step by step in increasing ethanol concentrations and critically dried with a K850CPD 2 M processor (Strumenti S.r.l., Roma, Italy). Afterward, samples were mounted on aluminum stubs and coated with a 10 nm layer of gold. Specimens were observed with a VEGA3-Tescan-type LMU microscope (Tescan Orsay Holding, a.s., Brno, Czech Republic), at a 20 kV voltage.

To perform an in-depth micromorphological comparison between the flowers of the three taxa, we grouped the trichome types in classes based on (1) the number of cells in the pedicel/head, (2) generic head and pedicel shape, (3) generic trichome size. Morphometric data were obtained by measuring trichome cell size ($n=3-10$) with ImageJ. Depending on the trichome type, we collected data regarding Gland Equatorial Diameter (GED), Gland Polar Diameter (GPD), Stem Cell Length (SCL), Neck Cell Length (NCL), First Stem Cell Length (FSCL), Second Stem Cell Length (SSCL), Total Diameter (TD), Gland Height (GH), Average Cell Ray (ACR), Gland Diameter (GD). The descriptive terminology was adopted following Uphof (1962); Payne (1978); Cantino (1990), and Osman et al. (2012). The presence or absence of secondary metabolites was recorded for each type of trichome. To allow for an easier visualization and comparison of the results regarding the presence or absence of specific trichome groups, a short progressive code was assigned to each trichome class. A representation of all observed trichome classes is provided in Online Resource 1.

We then calculated Jaccard matrices using (a) the presence or absence of the trichome subtypes (see the legend below in Tab.1), in the calyx and/or in the corolla; (b) the presence or absence of the trichome

types and their responsiveness to the dyes, or presence/absence of secondary metabolites. Neighbor-Joining trees were built on the matrices using the software R (version 4.3.2, R Core Team 2022) with the packages ape 5.0 (Paradis and Schliep 2019) and phangorn 2.7.1. (Schliep 2011). As an outgroup for the tree, we included *Salvia dorisiana* Standl., using the same information on the presence/absence of the overmentioned trichome classes.

Data obtained from pollen grains measurements were analysed using one-way parametric Analysis of Variance (ANOVA) followed by pairwise comparisons (post hoc t-tests with Benjamini-Hockberg correction) for both the diameter in polar view (D-PV) and the P/E ratio in equatorial view. A preliminary check was performed, based on the normality test (Shapiro-Wilks) and Levene test for equality of variances, to support using a parametric approach to assess the variability among the three taxa based on pollen micromorphology. The significance level was set at 0.05. Data analyses were carried out in R environment.

DNA extraction, amplification and sequencing

Extraction of gDNA was performed starting from leaves by DNeasy Plant Kit (QIAGEN, Milan, Italy) following the manufacturer's instructions. Purified gDNA was checked for concentration and purity using a Qubit 2 Fluorometer and Qubit dsDNA HS Assay Kit (Invitrogen, Carlsbad, CA, USA). The genomic locus selected for DNA analysis was the Internal Transcribed Spacer (ITS), as described in Gorini et al. (2023). Standard PCR amplification was performed using Wonder taq Polymerase (Euro-Clone s.p.a., Milan, Italy) in a 25 μ L reaction according to the manufacturer's instructions using primer described by Gorini et al (2023) for *Ocimum basilicum*. PCR cycles consisted of an initial denaturation step for 5 min at 95 °C, followed by 35 cycles of denaturation (45 s at 95 °C), annealing (45 s at 55 °C), and extension (1 min at 72 °C), and, hence, a final extension at 72 °C for 7 min. Amplicon occurrence was assessed by electrophoresis on agarose gel using 1.5% agarose TAE gel, and amplicon length was measured by comparison against 100 bp ladder. Purified amplicons were bidirectionally sequenced using an ABI 3730XL automated sequencing machine (Applied Biosystems, ThermoFisher Scientific, Milano, Italy).

Table 1 List of the trichome types recorded in the basil flowers, trichome description and morphometric values. Data are average values obtained from 3–10 measurements per trichome type, \pm SDs. The abbreviations correspond to Gland Equatorial Diameter (GED), Gland Polar Diameter (GPD),

Stem Cell Length (SCL), Neck Cell Length (NCL), First Stem Cell Length (FSCL), Second Stem Cell Length (SSCL), Total Diameter (TD), Gland Height (GH), Average Cell Ray (ACR), Gland Diameter (GD)

<i>A = short capitate trichomes (monocellular stalk, monocellular head)</i>	
1	Small, sessile, dot-like. GED = $29.8 \pm 9 \mu\text{m}$; GPD = $14.3 \pm 4 \mu\text{m}$
2	Small stalk, round head; GED = $38 \pm 3.5 \mu\text{m}$; GPD = $37.1 \pm 3.8 \mu\text{m}$; SCL = $10.8 \pm 1.9 \mu\text{m}$
3	Small stalk, clavate head; GED = $42 \pm 3.3 \mu\text{m}$; GPD = $24 \pm 4.5 \mu\text{m}$; SCL = $8.7 \pm 1.6 \mu\text{m}$
4	Small stalk, oblate head; GED = $28.5 \pm 1 \mu\text{m}$; GPD = $20.5 \pm 1.5 \mu\text{m}$; SCL = $9 \pm 0.5 \mu\text{m}$
5	Small stalk, necked, clavate head; GED = $37.5 \pm 0.5 \mu\text{m}$; GPD = $25 \pm 0.5 \mu\text{m}$; NCL = $5 \pm 0 \mu\text{m}$; SCL = $9 \pm 0 \mu\text{m}$
<i>B = medium-sized capitate trichomes (monocellular stalk, monocellular head)</i>	
1	Medium-sized stalk, round head; GED = $54 \pm 7 \mu\text{m}$; GPD = $50.6 \pm 1.1 \mu\text{m}$; SCL = $58.3 \pm 7.6 \mu\text{m}$
2	Medium-sized stalk, clavate head; GED = $50.6 \pm 0.5 \mu\text{m}$; GPD = $39.6 \pm 0.5 \mu\text{m}$; SCL = $61.3 \pm 0.5 \mu\text{m}$
<i>C = capitate trichomes with pluricellular stalk and monocellular head</i>	
1	2–4-celled stalk, medium, round head; GED = $30 \pm 2.6 \mu\text{m}$; GPD = $30.6 \pm 0.5 \mu\text{m}$; FSCL = $33 \pm 1 \mu\text{m}$; SSCL = $36 \pm 1 \mu\text{m}$
<i>D = capitate trichomes with monocellular stalk and pluricellular head</i>	
1	2-celled head, small, sessile; TD = $29.5 \pm 2.3 \mu\text{m}$; GH = $14 \pm 2.3 \mu\text{m}$; ACR = $14 \pm 1.2 \mu\text{m}$
2	2-celled head, small stalk; TD = $31 \pm 1.7 \mu\text{m}$; GH = $18 \pm 1 \mu\text{m}$; ACR = $16 \pm 2.8 \mu\text{m}$; SCL = $6 \pm 0 \mu\text{m}$
3	2-celled head, crown-shaped (flattened) head; TD = $35 \pm 1.1 \mu\text{m}$; GH = $18.3 \pm 2.8 \mu\text{m}$; ACR = $18 \pm 3.3 \mu\text{m}$; SCL = $6 \pm 0 \mu\text{m}$
<i>E = peltate trichomes</i>	
1	4-celled head; GD = $66 \pm 5 \mu\text{m}$
2	6-celled head; GD = $67.3 \pm 3.8 \mu\text{m}$
3	8-celled head; GD = $80.8 \pm 4.7 \mu\text{m}$
4	8-celled head, rectangular-shaped elongated stalk; GED = $92.3 \pm 9 \mu\text{m}$; GPD = $63.6 \pm 15 \mu\text{m}$; SCL = $52 \pm 25.5 \mu\text{m}$
5	4-celled head, small; GD = $42.3 \pm 11 \mu\text{m}$
<i>F = 1-celled stalk non-glandular trichomes</i>	
1	Short/medium-sized, monocellular stalk; TL = $62.3 \pm 31.9 \mu\text{m}$
2	Pyramidal-shaped monocellular stalk; TL = $49.66 \pm 4 \mu\text{m}$
3	Hooked, monocellular stalk; TL = $35.3 \pm 1.1 \mu\text{m}$
<i>G = pluricellular-stalked non-glandular trichomes</i>	
1	2-celled stalk; TL = $125 \pm 46 \mu\text{m}$
2	2-celled stalk, pyramidal shaped/hooked; TL = $191 \pm 41.2 \mu\text{m}$
3	Medium/large; 3–4 celled stalk; TL = $354.2 \pm 55.5 \mu\text{m}$
4	> 4 celled-stalk; TL = $488.1 \pm 85 \mu\text{m}$

Each sequence's 3' and 5' terminal portions were clipped to generate consensus sequences for each sample. After manual editing, primer removal, and

pairwise alignment, the sequences obtained were subjected to an individual Basic Local Alignment Search Tool (BLAST) in GenBank to verify their

taxonomic identity. All the sequences obtained were submitted to the GeneBank database (<https://www.ncbi.nlm.nih.gov>). A neighbour-joining (NJ) tree of the sequences obtained in this study and *Salvia dorisiana* as the outgroup was generated using MEGA 11—options=tree inference method: neighbour-joining; phylogeny test and options: bootstrap (1000 replicates); gaps / missing data: pairwise deletion; substitution model: p-distance; substitutions to include: transitions + transversions.

Results

Comparative flower macro- and micromorphology

From a macroscopic perspective, the three taxa under investigation exhibited differences in the anthocyanin pattern of corolla and calyx (Fig. 1a–f): considering the corollas, the white *O. × africanum* (Fig. 1a) resulted as the most recognizable. In contrast, ‘Cinnamon’ and ‘Blue Spice’ were more similar in colour to each other, both having whitish tones at the tube’s base, gradually transitioning into a pale violet hue at the top of the corolla (Fig. 1c, e). However, when examining the calyx, ‘Cinnamon’ appeared distinct due to its purplish calyx colour (Fig. 1d), which contrasted with the light green found in *O. × africanum* (Fig. 1b) and ‘Blue Spice’ (Fig. 1f). Additionally, in ‘Cinnamon’’s corolla, the non-glandular trichomes were pigmented with violet anthocyanins (not shown).

Micro- morphological analyses highlighted that the three basil taxa were distinguishable for the different trichome types’ presence, distribution and secondary metabolites composition.

Overall, the most frequently occurring elements were seven non-glandular and 16 glandular types of hairs (cfr. Online Resource 1; the list of the different classes and types together with morphometric data are indicated in the legend reported in Table 1, while the list of the trichomes found in each basil and their responsiveness to the dyes are provided in Table 2.

From the micromorphological point of view, The three basil taxa showed differences in the indumentums (see the Venn’s Diagram, Figs. 2, 3, 4 and 5) and different histochemical responses. All the non-glandular trichomes were shared except for the short type F1, which was not recorded in *O. × africanum*.

The pyramidal-shaped type F2 and the medium-sized F3 were always present uniquely in the calyx (Figs. 3a and 5a), where they were more frequently distributed on the margins or ribs (Figs. 3f and 6) F1 was found also in ‘Cinnamon’’s corolla. Pluricellular-stalked elements of type G were spread uniformly especially near the calyx’s base; they were disposed alternately to F types in the margins and were fewer in the central portion (Fig. 3a). These pluricellular trichomes were also present in the corolla, where they were abundant on the external surface of the central-distal portion of the upper lip but appeared as flagelliform (Fig. 5h). In non-glandular elements of *O. × africanum* and ‘Cinnamon’ (Figs. 3a and 6b), traces of lipids, polyphenols and mucopolysaccharides were also detected; traces of lipids were also found in the cytoplasm of some non-glandular trichomes of ‘Blue Spice’. Silicization patterns often ornamented the cell wall of all these elements (i.e. Figs. 6b and 5b).

The series of glandular types was more cultivar-specific than non-glandular ones (see Venn’s Diagram Fig. 2; Table 2). In the three cases, trichomes were more abundant and of more types in the calyx compared to the corolla (cfr. Fig. 5a and 6i); their distribution was almost uniform and did not follow any peculiar pattern (Fig. 5a, d–e, g–i). Only 7 of these types were also found in the corolla (upper lip mainly). Overall, short trichomes A3 (Figs. 3c, d, 5a (arrow), c and 6) and the peltate E1, E2 and E4 were shared by all the three taxa; short-sized elements D1, D2 and peltate E3 were in common only between *O. × africanum* and ‘Cinnamon’; only this latter and ‘Blue Spice’ shared the flattened/crown-shaped D3 (Fig. 3k); the medium-sized type B1 was shared only by *O. × africanum* and ‘Blue Spice’. Taxa-specific elements were: A5 in ‘Cinnamon’; A2 and C1 in *O. × africanum*; B2 and E5 in ‘Blue Spice’ (see Fig. 2).

Fluorol Yellow fluorescent dye highlighted that all taxa showed non-glandular trichomes with cutin / suberin in the cell walls (Fig. 6b).

Overall, the three basil taxa showed different histochemical patterns at the glandular trichome level (see Fig. 7). In *O. × africanum*, terpenoids and lipids were detected primarily in short-sized capitate A and peltate E trichomes. In some cases, dark brown cytoplasmic content was naturally present in the glands of the A elements. Instead, mucopolysaccharides, mucilage, and polyphenols were recorded more frequently

Table 2 Distribution of the trichome types and histochemistry in *Ocimum* × *africanum*, *O. basilicum* ‘Cinnamon’ and *O. basilicum* ‘Blue Spice’. The “+” sign indicates the occurrence of a trichome type in the plant organ, while a blank cell means absence

Species	Trichome type	Calyx	Corolla	Histochemical positivity	Autofluorescence/ pigment detected
<i>Ocimum</i> × <i>africanum</i>	A1	+		Fluorol yellow; Sudan III; Ruthenium Red	
	A2	+		Sudan III; Fluorol Yellow ±	Polyphenols
	A3	+	+	Ruthenium Red; TBO (polysaccharides); Sudan III; Fluorol yellow	
	B1	+			Chlorophyll
	C1	+		Ruthenium Red	
	D1	+		TBO (polyphenols/, flavonoids/tannins)	Polyphenols
	D2	+		Sudan III; TBO ± (polyphenols/flavonoids/ tannins)	
	E1	+	+	Ruthenium Red; Fluorol Yellow	Chlorophyll
	E2	+	+	Sudan III	
	E3	+	+	Ruthenium Red; TBO (polyphenols/flavo- noids/tannins)	Polyphenols
	E4	+		TBO ± (polyphenols/flavonoids/tannins)	
	F2	+		TBO ± (polyphenols/ flavonoids/tannins); Ruthenium Red ±; Fluorol Yellow	
	F3	+		Ruthenium Red ±; Fluorol Yellow	
	G1	+	+	Fluorol Yellow	
	G2	+		Sudan III ±; Rutheniu red ±; Fluorol Yellow	
	G3	+		Ruthenium Red ±; Fluorol Yellow	
	G3		+	Fluorol Yellow	
	H4	+		Sudan III ±; Fluorol Yellow	
	H4		+	Fluorol Yellow	
	<i>Ocimum basilicum</i> ‘Cin- namon’	A1	+		TBO ± (polyphenols/flavonoids/tannins)
A3		+		Sudan III; Fluorol Yellow	
A4		+		Fluorol Yellow	
A5		+		Ruthenium Red; Sudan III	
D1		+	+	Fluorol Yellow	Polyphenols
D2		+		Fluorol Yellow	Polyphenols
D3		+			
E1		+		TBO (polyphenols/flavonoids/tannins); Ruthe- nium Red	Polyphenols
E1			+	Sudan III; Ruthenium Red	
E2			+	TBO (polyphenols/flavonoids/tannins)	
E3		+		Sudan III	
E4		+		Fluorol Yellow	
F1		+	+	Fluorol Yellow	
F2		+		Fluorol Yellow	
F3		+		Fluorol Yellow	
G1		+	+	Fluorol Yellow	
G2		+	+	Fluorol Yellow	
G3		+	+	Fluorol Yellow	
G4		+	+	Fluorol Yellow	

Table 2 (continued)

Species	Trichome type	Calyx	Corolla	Histochemical positivity	Autofluorescence/ pigment detected
<i>Ocimum basilicum</i> 'Blue Spice'	A3	+		Fluorol Yellow	
	A3		+	Sudan III; Ruthenium Red	
	A4	+		Sudan III; Ruthenium Red	Fluorol yellow
	B1	+		Ruthenium Red	
	B2	+			Chlorophyll
	B2	+		Ruthenium Red	
	D3	+		Fluorol yellow; Ruthenium Red \pm	
	E1	+		Fluorol yellow	
	E2	+		Ruthenium Red	
	E2		+	TBO (polysaccharides)	
	E4	+		TBO (polysaccharides) TBO (polyphenols/ flavonoids/tannins); Ruthenium Red	
	E5	+		Ruthenium Red; TBO (polyphenols/flavo- noids/tannins); Sudan III	
	F1	+		Fluorol Yellow \pm	
	F2	+		Fluorol Yellow \pm ; Sudan III \pm	
	F3	+		Fluorol Yellow \pm	
	G1	+		Fluorol Yellow \pm ; Sudan III \pm	
	G2	+	+	Fluorol Yellow \pm ; Sudan III \pm	
	G3	+	+	Fluorol Yellow	
	G4	+		Fluorol Yellow	
	G4		+	Fluorol Yellow; Sudan III \pm	

in the capitate pluricellular stalked and monocellular headed C1 and in the monocellular stalked and pluricellular headed D types. Interestingly, in this taxon, the medium-sized B1 type found in calyx showed a glandular head that appeared green by transmission light (Fig. 3b), suggesting that chlorophyll pigments were present in the gland's head.

Also in 'Cinnamon' short-sized capitate A and peltate E trichomes showed lipids in the heads. These elements and trichomes of type D were also rich in terpenoids. Mucilage and mucopolysaccharides were found in other elements of type A and E; polyphenols were observed in subsessile glands A1, in pluricellular headed D, and in peltate E trichomes (Figs. 4d, c).

In 'Blue Spice', lipids/terpenoids were observed in some short-sized trichomes A, D, and peltate type E

in the calyx (Fig. 4d); lipids were found in one peltate and two types of short capitate trichomes; mucilage was recorded in two trichome types E. Polyphenols were observed in type E4 (Fig. 4c); overall, in 'Blue Spice', many elements (type B included) were rich in mucopolysaccharides. Some B2 trichomes that appeared green under transmission light were confirmed rich in chlorophyll pigments as observed for *O. x africanum* (Fig. 3b); however, other B2 elements with no green heads contained mucopolysaccharides.

The Neighbor-Joining trees were obtained with the Jaccard matrix, calculated a) on the presence or absence in the calyx or corolla of the 23 trichome types b) the content in secondary metabolites. In the first case, 46 morphological descriptors (23 for the calyx and 23 for the corolla) were used; in the second

Fig. 2 Venn's diagram showing the different trichome types shared by the three basil taxa

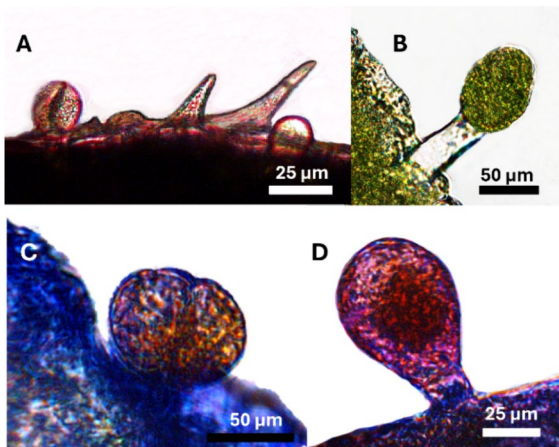
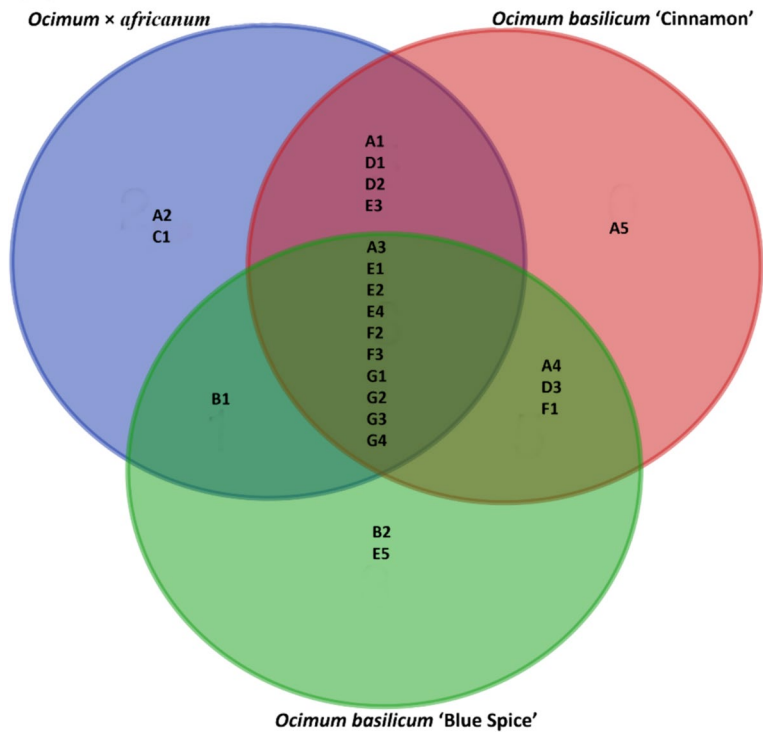


Fig. 3 Representative light microscopy micrographs of *Ocimum x africanum*. **A:** non-glandular and glandular trichomes, showing a slight positivity to Ruthenium Red; **B:** B1 trichome showing a chlorophyll content; **C:** a D1 trichome with a slight positivity to TBO; **D:** A3 trichome with a polysaccharidic content in the head

case, a final number of 164 characters was analysed. The resulting tree based only on morphological descriptors grouped 'Cinnamon' and *O. x africanum*

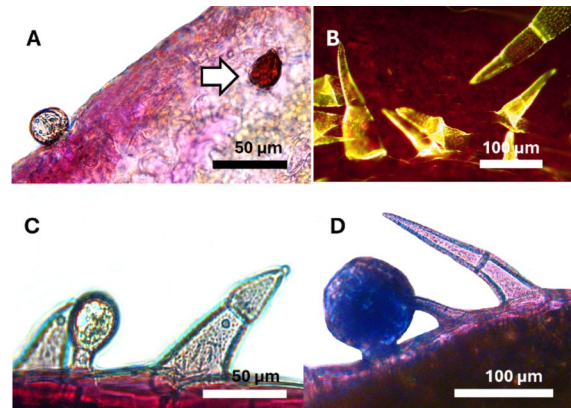


Fig. 4 Representative light microscopy micrographs of *Ocimum basilicum* 'Cinnamon'. **A:** View of the anthocyanized calyx surface, with a A1 subsessile trichome (arrow) and a D3 element; **B:** cutin-suberin content of the non-glandular trichomes, indicated by the positivity to Fluorol Yellow 088; **C:** an A2 short trichome and non-glandular elements; **D:** an E3 peltate trichome having a polyphenolic content as indicated by the positivity to TBO, and G trichomes

in the same cluster. At the same time, 'Blue Spice' was separated into a different branch (Fig. 8a). Based

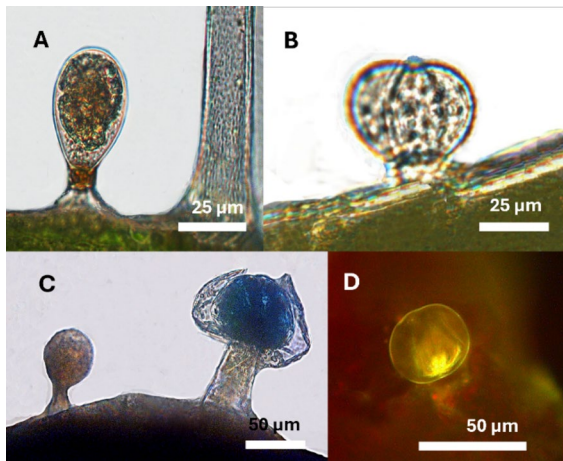


Fig. 5 Representative light microscopy micrographs of *O. basilicum* ‘Blue Spice’. **A**: an A5 trichome with a brown content in the head; **B**: detail of a D3 trichome; **C**: an A2 trichome and an elongated E4 trichome positive to TBO; **D**: J: short sized element, positive to Fluorol Yellow 088, showing a terpenoid/lipidic content

on chemical responsiveness, the tree distinguished all the taxa in three separate branches (Fig. 8b).

Comparative pollen micromorphology

The pollen grains of the three basil taxa were similar overall shape but showed differences in terms of apertures and size. Indeed, in all taxa, the shape of pollen grain was circular in the polar view and elliptic in the equatorial view ($P < E$). However, the pollen grains of *Ocimum* \times *africanum* were more frequently hexacolpate (87% ca.) and sometimes also octacolpate (13% ca.) (Fig. 9a), while ‘Cinnamon’ was characterized only by hexacolpate grains (Fig. 9b). Instead, in ‘Blue Spice’ the 40% of the pollen grains were octacolpate, the 30% heptacolpate and an equally 30% hexacolpate (Fig. 9c). Basic statistics of pollen grain measurements are reported in Table 3 together with the ANOVA results and the *post-hoc* test p-values. As highlighted, the ANOVA results showed significant differences between the three taxa for the D-PV values and the P/E ratio. At the 0.05 level, all the pairwise comparisons were also significant.

In all taxa, SEM analyses highlighted a bireticulate ornamentation of the tectum (Fig. 10a, c, e) and a psilate one for the colpus membrane (Fig. 10b, d, f). The bireticulate pattern comprised a primary

coarse-meshed reticulum, whose lumina were filled by a secondary fine-meshed reticulum. Muri of primary reticulum were angular, delimiting irregularly polygonal lumina, and appeared thicker in pollen grains of *Ocimum* \times *africanum* (Fig. 10a, b) in comparison to ‘Cinnamon’ (Fig. 10c, d) and ‘Blue Spice’ (Fig. 10e, f). The studied pollen grains were all heterobrochate, with lumina of different sizes.

DNA barcoding

Good DNA extraction yield (i.e., 20–40 ng/ μ L) were obtained from all the samples. Each barcode sequence was taxonomically assigned by using BLASTn analysis to the plant taxa with the nearest matches (maximum identity > 99% and query coverage of 100%). All the samples returned 100% maximum identity (with 100% query coverage). All the obtained sequences were submitted to GenBank (<https://www.ncbi.nlm.nih.gov>). Results are shown in Table 4.

Although DNA barcoding does not allow for the identification at the cultivar level, a Neighbour-joining tree has been constructed to verify the differences between the obtained sequences and identify any haplotypes. As can be seen from the generated tree, two haplotypes were identified. Specifically, the cultivar *O. basilicum* Blue Spice differs from the others two (*O. basilicum* ‘Cinnamomum’ and *O. \times africanum*).

Discussion

Nowadays, edible flowers are gaining popularity among consumers, who appreciate their taste, aroma, and pleasant aesthetic appearance. However, similar morphological characteristics may contaminate edible flowers with those of poisonous relatives (Matyjaszyk and Śmiechowska 2019). To avoid this risk, it is helpful to authenticate the plant material used. From this perspective, microscopic evaluation genetic techniques are useful and valuable tools for authenticating whole, cut, or powdered plant material even in commercial preparation (Ichim et al. 2020; Upton et al. 2020).

Although *O. basilicum* and many of its cultivars have been studied thoroughly from the point of view of the reproductive biology (Raju 1989), biochemistry and biological activity (Grayer et al. 1996; Javanmardi et al. 2002; Kwee et al. 2011; Prinsi et al. 2019;

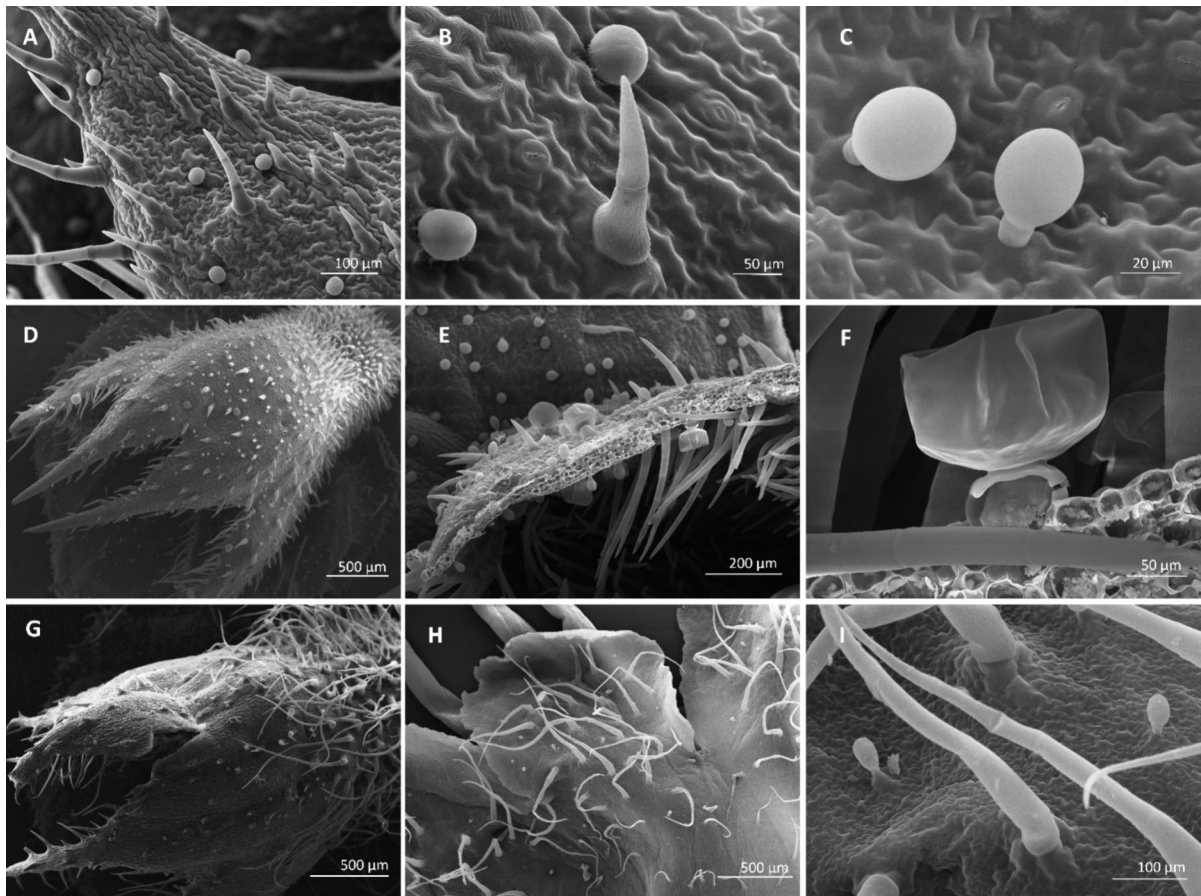


Fig. 6 Scanning electron microscopy micrographs of the calyx and corolla surfaces of the three basil taxa. **A–B:** *Ocimum* × *africanum*; **C–F:** *O. basilicum* ‘Cinnamon’; **G–I:** *O. basilicum* ‘Blue Spice’. **A:** distribution of the non-glandular G elements and short-sized capitate elements in the calyx; **B:** detail of H element and A1 trichomes in the calyx; **C:** A3 elements in the corolla; **D:** distribution of the non-glandular and glandular elements on the calyx external surface; view of the

calyx surfaces in which elongated peltate E elements are evident; **F:** detail of an elongated, rectangular-shaped E4 peltate trichome, in which the cytoplasmic content of the stalk is visible in the cross-section; **G:** distribution of the trichomes on the calyx surface; **H:** view of the corolla’s upper lip, in which short capitate trichomes are scattered among long non-glandular elements; **I:** detail of the corolla’s surface with A short trichomes and non-glandular hairs

Marchioni et al. 2020a; Rashid et al. 2023), information about morphology and micromorphology of the vegetative portions (Homa et al. 2016; Prinsi et al. 2019; Sanoj and Deepa 2021), breeding or molecular biology (Deschamps and Simon 2010; Dhar et al. 2020), and floral microscopical features are still lacking.

Through DNA barcoding analysis, as shown in Table 4, it was only possible to identify an organism at the species level. This is because the barcoding gap is not sufficient to distinguish samples at the cultivar level (Meier et al. 2008). For this reason, all samples were identified as *O. basilicum*. Nevertheless,

it was possible to distinguish two different haplotypes, one for samples *O. basilicum* ‘Cinnamon’ and *O. × africanum* and one for sample *O. basilicum* ‘Blue Spice’. In the literature, methodologies based on DNA have been presented to distinguish basil cultivars. For example, Ibrahim and colleagues (2013) have developed a method based on RAPD that could help in identifying genetic variation among different cultivars of basil. Other techniques, such as chloroplast sequencing or microsatellite analysis, could be useful methods for this purpose (Gupta et al. 2010; Xiao et al. 2021). However, these methodologies are

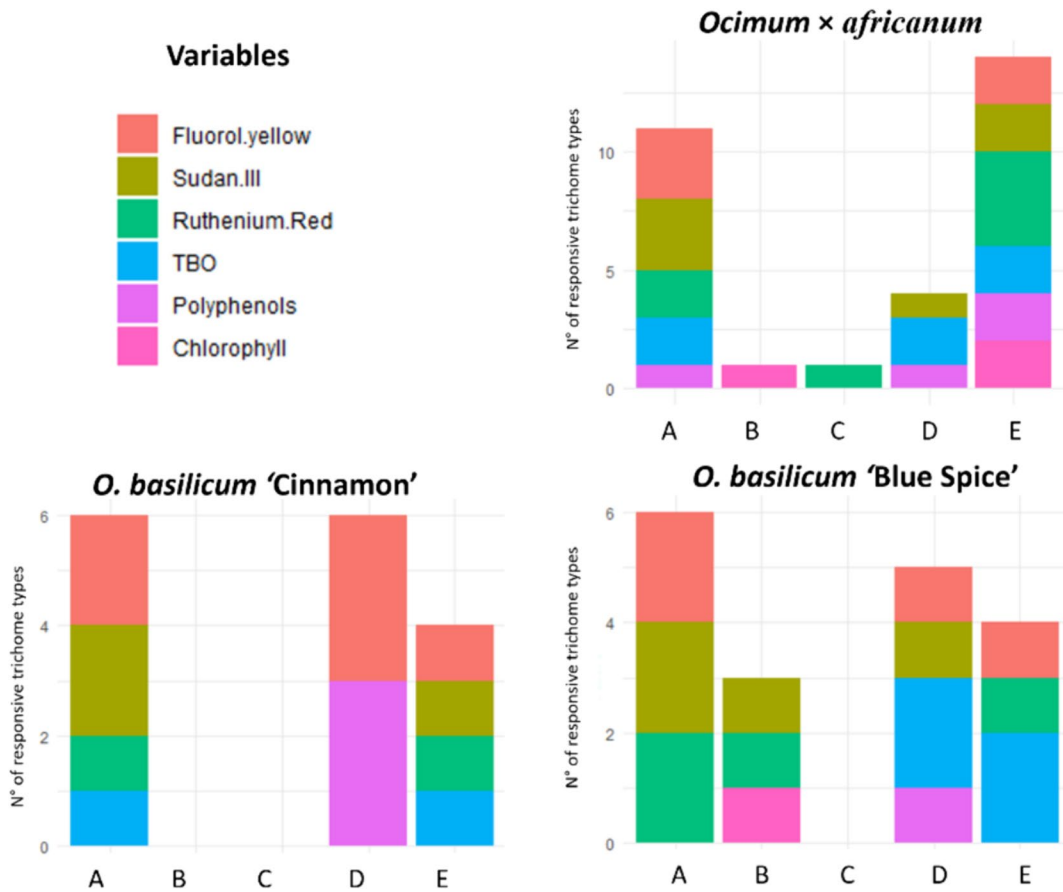


Fig. 7 Representation of the histochemical responsiveness patterns for the different glandular trichome classes. In each bar, the number of different trichome types found per class is

reported; the colours in the bar indicate how many trichomes in the class were showing a specific content in secondary metabolites

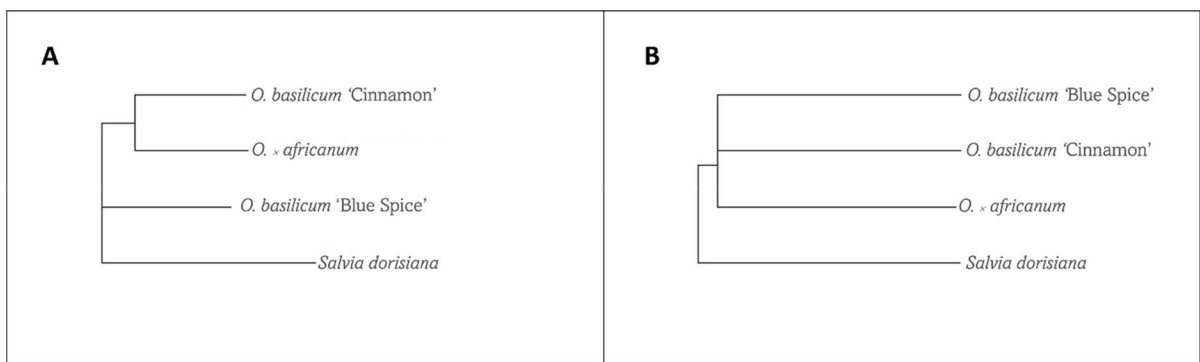


Fig. 8 Neighbor-Joining trees, obtained from Jaccard distances. **A:** tree calculated on the presence/absence of the 24 trichome morphotypes in the calyx and/or in the corolla; **B:** tree

calculated on the presence of the 24 morphotypes in the calyx and/or in the corolla and their histochemical positivites. *Salvia dorisiana* has been used as the outgroup

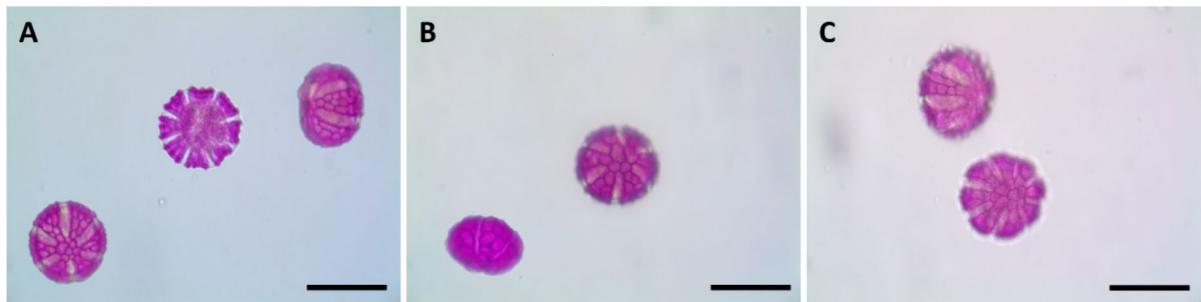


Fig. 9 Light microscopy micrographs of basil pollen grains: **A** *Ocimum* × *africanum*, with six or eight colpi; **B** *O. basilicum* ‘Cinnamon’, with six colpi; **C** *O. basilicum* ‘Blue Spice’, with eight colpi. Bar = 50 μm

Table 3 Diameter in polar view and P/E ratio of the pollen grains of the three taxa, shown as mean value (SD). Data were obtained from 30 different pollen grains, and then analysed with one-way ANOVA and post-hoc pairwise comparisons with Benjamini-Hockberg correction

Taxon	D-PV (μm) ^a	P/E ^b
<i>Ocimum</i> × <i>africanum</i>	56.65 (2.39)	0.765 (0.068)
<i>Ocimum basilicum</i> ‘Cinnamon’	52.07 (2.74)	0.721 (0.055)
<i>Ocimum basilicum</i> ‘Blue Spice’	54.67 (3.00)	0.677 (0.062)
ANOVA F-value	21.33	15.00
ANOVA p-value	<0.0001	<0.0001

^aD-PV: diameter in polar view. *p*-values of the post-hoc pairwise comparisons: *Ocimum* × *africanum* vs *O. basilicum* ‘Cinnamon’ 0.0006; *O. x africanum* vs *O. basilicum* ‘Blue Spice’ 0.0059; *O. basilicum* ‘Cinnamon’ vs *O. basilicum* ‘Blue Spice’ <0.0001.

^bP/E: ratio between polar and equatorial axis. *p*-values of the post-hoc pairwise comparisons: *Ocimum* × *africanum* vs *O. basilicum* ‘Cinnamon’ 0.0083; *O. x africanum* vs *O. basilicum* ‘Blue Spice’ <0.0001; *O. basilicum* ‘Cinnamon’ vs *O. basilicum* ‘Blue Spice’ 0.0083

expensive and not universally applicable, requiring specific optimization for basil.

Although the cultivar level was not reachable through molecular tools, micromorphological and histochemical differences supporting the discrimination of the specimens were found, and the sites of production of secondary metabolites with known bioactive properties and nutritional value such as polyphenols, lipids/terpenoids and polysaccharides were characterised.

Previously, Marchioni et al. (2020a) indicated that, considering the biochemistry, carotenoids are the most abundant pigments in these cultivars. According

to our results, the anthocyanin pigments contributing to the violet patterns of the calyx and corolla constitute the most important characters for the identification of Cinnamon’s flowers from Blue Spice and *O. x africanum* at the macroscopic level.

All the basils displayed only uniseriate trichomes. A total of 23 morphotypes, including non-glandular and glandular hairs and distinguishable by the shape, number of cells in the stalk/head and the size, was found by screening the adaxial and abaxial surfaces of the calyx and the adaxial surface of the petals, similarly to what performed by Dos Santos Tozin and Rodrigues (2019) for *Ocimum gratissimum* L. Consistent with what observed by these authors and by Werker (1993), who investigated leaf characteristics, we found both capitate and peltate glandular trichomes in the corolla and calyx tissues, although the abundance was different depending on the tissue considered. Glandular trichomes were more abundant on the calyx respect to the corolla in all the three taxa, similarly to what observed for other Lamiaceae (Dos Santos Tozin and Rodrigues 2019): the corolla mainly showed short type A trichomes and the peltate E elements, confirming that the secretory activity aiming at the emission of fragrances, at preventing water evaporation and at avoiding herbivory is mainly exerted by the green tissues than those of the corolla (Fahn 2000; Tian et al. 2017).

Many of the trichome types recognized have been already reported in Lamiaceae. Different types of capitate elements have been recorded in the family, including trichomes with stalks of different length (Werker et al. 1985a, 1985b). However, only short capitate types have been studied in detail, with their ultrastructure and histochemistry

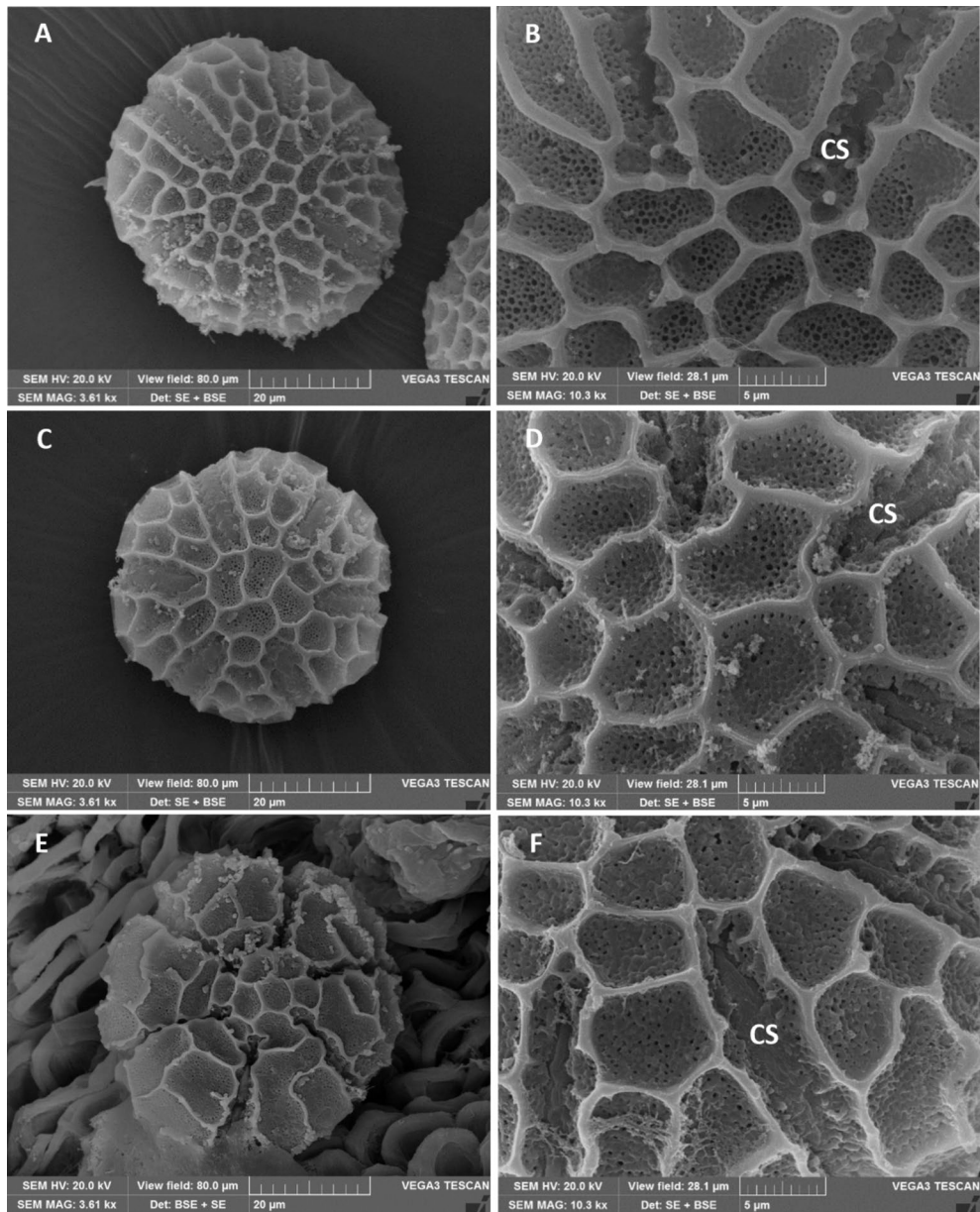


Fig. 10 Scanning electron microscopy micrographs of basil pollen grains: *Ocimum* × *africanum* (A–B), *O. basilicum* ‘Cinnamon’ (C–D), *O. basilicum* ‘Blue Spice’ (E–F). A, C, E:

polar view; B, D, F: magnification of surface ornamentation with colpi. CS: colpus surface

Table 4 DNA barcoding results. The table shows the declared taxa, resulting taxon, origin, collection year, and accession numbers deposited in the Genbank database (<https://www.ncbi.nlm.nih.gov>)

Declared taxon	Species resulting	Origin	Collection year	Accession number
<i>Ocimum basilicum</i> ‘Cinnamon’	<i>Ocimum basilicum</i>	Italy	2019	OR161824
<i>Ocimum</i> × <i>africanum</i>	<i>Ocimum basilicum</i>	Italy	2019	OR161825
<i>Ocimum basilicum</i> ‘Blue Spice’	<i>Ocimum basilicum</i>	Italy	2019	OR161826

suggesting the occurrence of polysaccharidic secretions (Giuliani and Maleci Bini 2008 and references therein). Medium-sized capitate elements, for which we haven't observed the neck cell, seem to be similar to the trichomes described by Rusydi et al. (2013), Giuliani and Maleci Bini (2008), and Thi Tran et al. (2022). The presence of essential oil in these elements was discussed by Giuliani and Maleci Bini (2008): in our study, we found a polysaccharidic content, and chlorophyll in rare cases (see Fig. B). Although the stalk was not visible, the A1 glands that we recorded were named as sessile by Cantino (1990), who stated that the short pedicel cell could be recognized in the transversal section.

All the peltate morphotypes that we observed have been previously described in the literature (i.e. see Cantino 1990). Peltate trichomes are known as the main site of the production and storage of the EOs (Fahn 2000 and references therein; Giuliani and Maleci Bini 2008 and references therein). To our knowledge, a morphotype similar to the elongated peltate type E4 shared by the three cultivars has been found in *Lavandula pinnata* by Huang et al. (2008), in *Stachys germanica* subsp. *salviifolia* by Giuliani and Maleci Bini (2008), in *Salvia smyrnea* by Baran et al. (2010) and in *S. chrysophylla* by Kahraman et al. (2010), albeit in our case the cuticle and the pedicel appeared as more rectangular-shaped and square. Possibly deriving from the presence or absence of specific peltate types, differences in the spectra of volatile compounds (specifically, different abundances of sesquiterpene hydrocarbons) have been found in the flower of these taxa, sampled in the same location, by Marchioni et al. (2020a).

The presence of chlorophyll, apart from B trichomes in 'Blue Spice' and *O. × africanum*, was recorded in this latter also in the peltate E1 element. Interestingly, according to the literature, this is the first report of chlorophyll in the glands for Lamiaceae: photosynthetic glandular trichomes are instead known to occur in *Nicotiana tabacum* (Keene and Wagner 1985; Laterre et al. 2017).

The tree based on only morphological characters suggested a slightly higher similarity between *O. × africanum* and 'Cinnamon' than 'Blue Spice' (Fig. 5a), similarly to what observed in the tree built on molecular characters (Fig. 11) The three taxa could be discriminated by the occurrence of taxon-specific elements (see Fig. 2). The pluricellular-stalked and

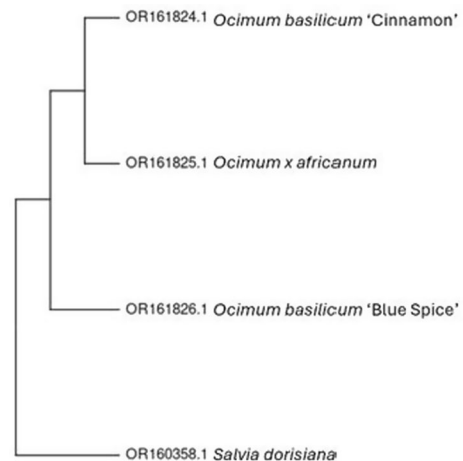


Fig. 11 Neighbour-joining tree based on internal transcribed spacer 2 (ITS2) sequences of *Ocimum* species generated with Mega. *Salvia dorisiana* has been used as the outgroup

monocellular headed C elements could only be found in 'Blue Spice'; type B trichomes were absent in 'Cinnamon'. Only 'Cinnamon' showed the necked short elements A5. In addition to the presence or absence of the morphotypes, there were cases in which the same trichome types replied differently to the dyes used depending on the taxa, or showed a different content in secondary metabolites as assessed by autofluorescence analyses. The secretion of different compounds depending on the trichome morphotype has been already in *O. gratissimum* by Dos Santos Tozin and Rodrigues (2019). Although we could recognize only the macro-groups of compounds and we have no data about the identity of the molecules secreted by the glands, it is likely that these factors, taken together, may result in the chemical diversity previously described for these taxa (i.e. Grayer et al. 1996; Marchioni et al. 2020a). For instance, while the morphotype E4 had a lipophilic content in 'Cinnamon', a mucilaginous/hydrophilic content was observed for the same trichome type in 'Blue Spice' and *O. × africanum*, indicating the possible expression of different genes for the biosynthesis of secondary metabolites. The chemical diversity patterns were also confirmed by the splitting of the taxa into three separate clades in the tree (Fig. 5b). In addition to the morphology of trichomes and their content of bioactive compounds, also pollen data provided significant results useful for the distinction of the three basilis at the taxonomic

level. This is the first study that compares the pollen micromorphology of *Ocimum* × *africanum*, *O. basilicum* ‘Cinnamon’, and *O. basilicum* ‘Blue Spice’. The identification of pollen traits is important because these edible flowers are widely used to flavour salads and other dishes. Due to the small size of basil flowers, they are ingested together with the reproductive organs, including the anthers and pollen. Therefore, even the characteristics of the pollen are useful traits for the correct identification of edible flowers intended for human consumption.

Light microscopy analyses highlighted that there were some differences among the pollen grains, even if they looked similar. Firstly, the taxa showed a different number of colpi: six in ‘Cinnamon’, six or eight in *O. × africanum*, and from six to eight in ‘Blue Spice’. Secondly, they resulted significantly different regarding the size, with ‘Blue Spice’ pollen grains having the highest D-PV and ‘Cinnamon’ the smallest one. Moreover, considering the mean value of the P/E ratio and the classification of Erdtman (1952), *O. × africanum* pollen grains could be classified as suboblate, while the grains of the other two taxa were oblate. Overall, all pollen grains fell into the category of size called “large” (51–100 µm) according to Kremp (1965). The same has been observed in *O. basilicum* by Gul et al. (2019); Bahadur et al. (2022), and Kumari et al. (2022).

Based on the descriptions carried out by Harley et al. (1992) on tribe Ocimeae, the pollen grains of the three taxa could be described as Pollen Type II, characterized by a P/E ratio of 0.92–0.65 and an oblate or suboblate shape. In particular, our samples corresponded to the Subtype IIA, showing a secondary reticulum densely perforate as detected by SEM analysis. All taxa showed the same exine ornamentation. The tectum surface of *O. basilicum* was described as “doubly reticulate/bireticulate” by Harley et al. (1992) and Bahadur et al. (2022), while in other research it was called “mega reticulate” (Doaigey et al. 2018; Bahadur et al. 2022). However, in both cases the term referred to the presence of an outer reticulum and an infrareticulum.

Conclusion

In conclusion, we compared the morphological, histochemical and molecular characteristics between

the edible flowers of three basil taxa. The sequences obtained with the DNA barcoding approach were deposited in GenBank and clearly allowed for the identification of the samples as *Ocimum basilicum*; one haplotype for *O. basilicum* ‘Cinnamon’ and *O. × africanum* and one *O. basilicum* ‘Blue Spice’. However, further analyses are needed to obtain molecular markers suitable for basil cultivars and hybrids identification. On the other hand, micromorphological analyses of the indumentums and pollen grains allowed to obtain information regarding the sites of production of potentially beneficial secondary metabolites, and revealed unique characteristics which can be used as a reference to discriminate the taxa between each other. Among these, the most informative characters were taxon-specific trichomes, the absence of certain trichome classes depending on the taxa, the number of colpi and the size of the pollen.

Acknowledgements This experimental study was performed in the framework of the PhD project of Federica Betuzzi (PhD School in Science and Technologies for the Earth and Environment, curriculum Biology Applied to Agriculture and the Environment, XXXIX cycle, University of Genoa), granted by the Ministry of University and Research. We thank Mrs. Laura Negretti for SEM technical assistance.

Author contributions Laura Cornara, Miriam Bazzicalupo, Andrea Copetta and Jessica Frigerio conceived and designed the study. Material preparation was performed by Andrea Copetta, Miriam Bazzicalupo, Jessica Frigerio and Federica Betuzzi. Data collection was performed by Miriam Bazzicalupo, Federica Betuzzi, Werther Guidi Nissim and Jessica Frigerio. Data analysis was performed by Miriam Bazzicalupo, Federica Betuzzi, Jessica Frigerio, Werther Guidi Nissim and Fabio Rapallo. The first draft of the manuscript was prepared by Miriam Bazzicalupo, Andrea Copetta, Federica Betuzzi, Jessica Frigerio and Laura Cornara. All authors read and approved the final manuscript.

Funding Open access funding provided by Università degli Studi di Milano - Bicocca within the CRUI-CARE Agreement. This research received no external fundings.

Data availability No datasets were generated or analysed during the current study.

Declarations

Conflict of interest The authors declare no competing interests.

Open Access This article is licensed under a Creative Commons Attribution 4.0 International License, which permits use, sharing, adaptation, distribution and reproduction in any

medium or format, as long as you give appropriate credit to the original author(s) and the source, provide a link to the Creative Commons licence, and indicate if changes were made. The images or other third party material in this article are included in the article's Creative Commons licence, unless indicated otherwise in a credit line to the material. If material is not included in the article's Creative Commons licence and your intended use is not permitted by statutory regulation or exceeds the permitted use, you will need to obtain permission directly from the copyright holder. To view a copy of this licence, visit <http://creativecommons.org/licenses/by/4.0/>.

References

- Ali M, Liu YJ, Xia QP, Bahadur S, Hussain A, Shao JW, Shuaib M (2021) Pollen micromorphology of eastern Chinese *Polygonatum* and its role in taxonomy by using scanning electron microscopy. *Microsc Res Tech* 84:1451–1461. <https://doi.org/10.1002/jemt.23701>
- Al-Kateb H, Mottram DS (2014) The relationship between growth stages and aroma composition of lemon basil *Ocimum citriodorum* Vis. *Food Chem* 152:440–446. <https://doi.org/10.1016/j.foodchem.2013.12.001>
- Arogundade OO, Adedeji O (2009) Pollen grain morphology of three species and a variety of *Ocimum* Linn. (Lamiaceae) in Southwestern Nigeria. *J Sci Technol*. <https://doi.org/10.4314/jst.v29i3.50028>
- Azzazy M (2019) Micromorphology of pollen grains, trichomes of sweet basil. *Egypt Adv Complement Alt Med* 5:427–433. <https://doi.org/10.31031/ACAM.2019.05.000604>
- Bahadur S, Taj S, Ahmad M, Zafar M, Gul S, Shuaib M, Butt MA, Hanif U, Nizamani MM, Hussain F, Romman M (2022) Authentication of the therapeutic Lamiaceae taxa by using pollen traits observed under scanning electron microscopy. *Microsc Res Tech* 85:2026–2044. <https://doi.org/10.1002/jemt.24061>
- Bano A, Rashid S, Ahmad M, Bhatti GR, Yaseen G, Anjum F, Ahmed SN, Zafar M, Asma M, Sultana S, Adeel M, Ozdemir FA, Kilic O (2020) Comparative pollen and foliar micromorphological studies using light microscopy and scanning electron microscopy of some selected species of Lamiaceae from Alpine Zone of Deosai Plateau, Western Himalayas. *Microsc Res Tech* 83:579–588. <https://doi.org/10.1002/jemt.23448>
- Baran P, Aktas K, Özdemir C (2010) Structural investigation of the glandular trichomes of endemic *Salvia smyrnaea* L. *S Afr J Bot* 76:572–578
- Beatovic D, Krstic-Milosevic D, Trifunovic S, Siljegovic J, Glamoclija J, Ristic M, Jelacic S (2015) Chemical composition, antioxidant and antimicrobial activities of the essential oils of twelve *Ocimum basilicum* L. cultivars grown in Serbia. *Rec Nat Prod* 1:62
- Bhattacharjee R (1980) Taxonomic studies in *Stachys* II: a new infrageneric classification of *Stachys* L. *Notes Roy Bot Gard Edinb* 38:65–96
- Bhattacharjee R (1982) *Stachys* L. In: Davis PH (ed) *Flora of Turkey and the East Aegean Islands*, vol 7. Edinburgh University Press, Edinburgh, pp 199–262
- Bini Maleci L, Servettaz O (1991) Morphology and distribution of trichomes in Italian species of *Teucrium* sect. *Chamaedrys* (Labiatae)—a taxonomical evaluation. *Plant Syst Evol* 174:83–91
- Brechbill GO (2007) *Classifying Aroma Chemicals*. Fragrance Books Inc., New Jersey
- Brundrett MC, Kendrick B, Peterson CA (1991) Efficient lipid staining in plant material with sudan red 7B or fluoral [correction of fluoral] yellow 088 in polyethylene glycol-glycerol. *Biotech Histochem* 66:111–116. <https://doi.org/10.3109/10520299109110562>
- Cantino PD (1990) The phylogenetic significance of stomata and trichomes in the Labiatae and Verbenaceae. *J Arnold Arbor* 71:323–370
- Chieco C, Rotondi A, Morrone L, Rapparini F, Baraldi R (2013) An ethanol-based fixation method for anatomical and micro-morphological characterization of leaves of various tree species. *Biotech Histochem* 88:109–119
- Copetta A, Lingua G, Berta G (2006) Effects of three AM fungi on growth, distribution of glandular hairs, and essential oil production in *Ocimum basilicum* L. var. *Genovese Mycorrhiza* 16:485–494. <https://doi.org/10.1007/s00572-006-0065-6>
- Cornara L, Smeriglio A, Frigerio J, Labra M, Di Gristina E, Denaro M, Mora E, Trombetta D (2018) The problem of misidentification between edible and poisonous wild plants: reports from the Mediterranean area. *Food Chem Toxicol* 119:112–121
- Deschamps C, Simon JE (2010) Phenylpropanoid biosynthesis in leaves and glandular trichomes of basil (*Ocimum basilicum* L.). *Methods Mol Biol* 643:263–273. https://doi.org/10.1007/978-1-60761-723-5_18
- Dhar N, Sarangapani S, Reddy VA, Kumar N, Panicker D, Jin J, Chua N-H, Sarojam R (2020) Characterization of a sweet basil acyltransferase involved in eugenol biosynthesis. *J Exp Bot* 71(12):3638–3652. <https://doi.org/10.1093/jxb/eraa142>
- Doaigey AR, El-Zaidy M, Alfarhan A, Milagy AE, Jacob T (2018) Pollen morphology of certain species of the family Lamiaceae in Saudi Arabia. *Saudi J Biol Sci* 25:354–360
- Dos Santos Tozin LR, Rodrigues TM (2019) Glandular trichomes in the tree-basil (*Ocimum gratissimum* L. Lamiaceae): Morphological features with emphasis on the cytoskeleton. *Flora* 259:151459
- Dudai N, Nitzan N, Gonda I (2020) *Ocimum basilicum* L (Basil). In: Novak J, Blüthner WD (eds) *Medicinal Aromatic and Stimulant Plants Handbook of Plant Breeding*, vol 12. Springer, Cham
- Erdtman G (1952) *Pollen morphology and plant taxonomy. An introduction to palynology*. Almquist and Wiksell, Stockholm
- Fahn A (2000) Structure and function of secretory cells. In: Hallahan DL, Gray JC (eds) *Advances in botanical research Plant trichomes*. Academic Press, pp 37–75
- Fernandes L, Ramalhosa E, Pereira JA, Saraiva JA, Casal S (2018) The unexplored potential of edible flowers lipids. *Agriculture* 8:146

- Fischer R, Nitzan N, Chaimovitch D, Rubin B, Dudai N (2011) Variation in essential oil composition within individual leaves of sweet basil (*Ocimum basilicum* L.) is more affected by leaf position than by leaf age. *J Agric Food Chem* 59:4913–4922. <https://doi.org/10.1021/jf200017h>
- Frigerio J, Gorini T, Galimberti A, Bruni I, Tommasi N, Mezzasalma V, Labra M (2019) DNA barcoding to trace Medicinal and Aromatic Plants from the field to the food supplement. *J Appl Bot Food Qual* 92:33–38
- Frigerio J, Agostinetto G, Mezzasalma V, De Mattia F, Labra M, Bruno A (2021) DNA-based herbal teas' authentication: an ITS2 and *psbA-trnH* Multi-Marker DNA metabarcoding approach. *Plants* 10:2120. <https://doi.org/10.3390/plants10102120>
- Galimberti A, Bruno A, Mezzasalma V, De Mattia F, Bruni I, Labra M (2015) Emerging DNA-based technologies to characterize food ecosystems. *Food Res Int* 69:424–433
- Gang DR, Wang J, Dudareva N, Nam KH, Simon JE, Lewinsohn E, Pichersky E (2001) An investigation of the storage and biosynthesis of phenylpropanes in sweet basil. *Plant Physiol* 125:539–555. <https://doi.org/10.1104/pp.125.2.539>
- Giuliani C, Maleci Bini L (2008) Insight into the structure and chemistry of glandular trichomes of Labiatae, with emphasis on subfamily Lamioideae. *Plant Syst Evol* 276:199–208
- Gorini T, Mezzasalma V, Deligia M, De Mattia F, Campone L, Labra M, Frigerio J (2023) Check your shopping cart: DNA barcoding and mini-barcoding for food authentication. *Foods* 12:2392
- Grayer RJ, Kite GC, Goldstone FJ, Bryan SE, Paton A, Putievsky E (1996) Intraspecific taxonomy and essential oil chemotypes in sweet basil, *Ocimum basilicum*. *Phytochemistry* 43:1033–1039
- Grazina L, Amaral JS, Mafra I (2020) Botanical origin authentication of dietary supplements by DNA-based approaches. *Compr Rev Food Sci Food Saf* 19:1080–1109
- Gul S, Ahmad M, Zafar M, Bahadur S, Sultana S, Begum N, Shah SN, Zaman W, Ullah F, Ayaz A, Hanif U (2019) Taxonomic study of subfamily Nepetoideae (Lamiaceae) by polynomorphological approach. *Microsc Res Tech* 82:1021–1031. <https://doi.org/10.1002/jemt.23249>
- Gupta S, Shukla R, Roy S, Sen N, Sharma A (2010) In Silico SSR and FDM analysis through EST sequences in *Ocimum basilicum*. *Plant Omics* 3:121–128
- Harley MM, Paton A, Harley RM, Cade PG (1992) Pollen morphological studies in tribe Ocimeae (Nepetoideae: Labiatae): I. *Ocimum* L. *Grana* 31(3):161–176. <https://doi.org/10.1080/00173139209432027>
- Homa K, Barney WP, Ward DL, Wyenandt CA, Simon JE (2016) Morphological characteristics and susceptibility of basil species and cultivars to *Peronospora belbahrii*. *HortScience* 51:1389–1396
- Huang SS, Kirchoff BK, Liao JP (2008) The capitata and pelate glandular trichomes of *Lavandula pinnata* L. (Lamiaceae): histochemistry, ultrastructure, and secretion. *J Torrey Bot Soc* 135:155–167
- Husti A, Cantor M, Buta E, Horț D (2013) Current trends of using ornamental plants in culinary arts. *ProEnvironment* 6:52–58
- Ichim MC, Häser A, Nick P (2020) Microscopic authentication of commercial herbal products in the globalized market: potential and limitations. *Front Pharmacol* 11:876. <https://doi.org/10.3389/fphar.2020.00876>
- Javanmardi J, Khalighi A, Kashi A, Bais HP, Vivanco JM (2002) Chemical characterization of basil (*Ocimum basilicum* L.) found in local accessions and used in traditional medicines in Iran. *J Agric Food Chem* 50:5878–5883. <https://doi.org/10.1021/jf020487q>
- Kahraman A, Celep F, Dogan M (2010) Anatomy, trichome morphology and palynology of *Salvia chrysophylla* Stapf (Lamiaceae). *S Afr J Bot* 76(2):187–195
- Karousou R, Bosabalidis AM, Kokkini S (1992) *Sideritis syriaca* ssp. *syriaca*: Glandular trichome structure and development in relation to systematics. *Nord J Bot* 12:31–37. <https://doi.org/10.1111/j.1756-1051.1992.tb00198.x>
- Keene CK, Wagner GJ (1985) Direct demonstration of divatrienediol biosynthesis in glandular heads of tobacco trichomes. *Plant Physiol* 79:1026–1032. <https://doi.org/10.1104/pp.79.4.1026>
- Kraus JE, de Sousa HC, Rezende MH, Castro NM, Vecchi C, Luque R (1998) Astra blue and basic Fuchsin double staining of plant materials. *Biotech Histochem* 73:235
- Kremp OW (1965) *Morphologic Encyclopedia of Palynology*. University of Arizona Press
- Kress WJ, Erickson DL (2007) A two-locus global DNA barcode for land plants: The coding *rbcL* gene complements the non-coding *trnH-psbA* spacer region. *PLoS ONE* 2(6):e508. <https://doi.org/10.1371/journal.pone.0000508>
- Kumari M, Prasad A, Rahman LU, Kumar Mathur A, Mathur A (2022) In vitro germination, storage and microscopic studies of pollen grains of four *Ocimum* species. *Ind Crops Prod* 177:114445. <https://doi.org/10.1016/j.indcrop.2021.114445>
- Kwee EM, Niemeyer ED (2011) Variations in phenolic composition and antioxidant properties among 15 basil (*Ocimum basilicum* L.) cultivars. *Food Chem* 128:1044–1050. <https://doi.org/10.1016/j.foodchem.2011.04.011>
- Laterre R, Pottier M, Remacle C, Boutry M (2017) Photosynthetic trichomes contain a specific Rubisco with a modified pH-dependent activity. *Plant Physiol* 173:2110–2120. <https://doi.org/10.1104/pp.17.00062>
- Laura M, Forti C, Barberini S, Ciorba R, Mascarello C, Giovannini A, Pistelli L, Pieracci Y, Lanteri AP, Ronca A et al (2023) Highly efficient CRISPR/Cas9 mediated gene editing in *Ocimum basilicum* 'FT Italiko' to induce resistance to *Peronospora belbahrii*. *Plants* 12:2395. <https://doi.org/10.3390/plants12132395>
- Majdi C, Pereira C, Dias MI, Calhelha RC, Alves MJ, Rhourri-Frih B, Charrouf Z, Barros L, Amaral JS, Ferreira ICFR (2020) Phytochemical characterization and bioactive properties of Cinnamon Basil (*Ocimum basilicum* cv. 'Cinnamon') and Lemon Basil (*Ocimum* × *citriodorum*). *Antioxidants* 9:369. <https://doi.org/10.3390/antiox9050369>
- Makri O, Kintzios S (2008) *Ocimum* sp. (Basil): botany cultivation, pharmaceutical properties, and biotechnology. *J Herbs Spices Med Plants* 13(3):123–150. https://doi.org/10.1300/J044v13n03_10

- Marchioni I, Najar B, Ruffoni B, Copetta A, Pistelli L, Pistelli L (2020a) Bioactive compounds and aroma profile of some Lamiaceae edible flowers. *Plants* 9:691
- Marchioni I, Pistelli L, Ferri B, Copetta A, Ruffoni B, Pistelli L, Najar B (2020b) Phytonutritional content and aroma profile changes during postharvest storage of edible flowers. *Front Plant Sci* 11:590968. <https://doi.org/10.3389/fpls.2020.590968>
- Matyjaszczyk E, Śmiechowska M (2019) Edible flowers. Benefits and risks pertaining to their consumption. *Trends Food Sci Technol* 91:670–674. <https://doi.org/10.1016/j.tifs.2019.07.017>
- Maurya S, Sangwan NS (2019) Profiling of essential oil constituents in *Ocimum* Species. *Proc Natl Acad Sci India Sect B Biol Sci* 26:1–7
- Meier R, Zhang G, Ali F (2008) The use of mean instead of smallest interspecific distances exaggerates the size of the “barcoding gap” and leads to misidentification. *Syst Biol* 57:809–813
- Mlcek J, Rop O (2011) Fresh edible flowers of ornamental plants—A new source of nutraceutical foods. *Trends Food Sci Technol* 22:561–569
- Mohammed Abubakar B, Mohd Salleh F, Shamsir Omar MS, Wagiran A (2017) Review: DNA barcoding and chromatography fingerprints for the authentication of botanicals in herbal medicinal products. *Evid Based Compl Alt* 1:28. <https://doi.org/10.1155/2017/1352948>
- Nabila AM, Zafar M, Bahadur S, Sultana S, Taj S, Celep F, Majeed S, Rozina, (2022) Palynomorphological diversity among the Asteraceous honeybee flora: An aid to the correct taxonomic identification using multiple microscopic techniques. *Microsc Res Tech* 85:570–590. <https://doi.org/10.1002/jemt.23932>
- Najar B, Marchioni I, Ruffoni B, Copetta A, Pistelli L, Pistelli L (2019) Volatilomic analysis of four edible flowers from *Agastache* Genus. *Molecules* 24:4480. <https://doi.org/10.3390/molecules24244480>
- Navarro T, El Oualidi J (2000) Trichome morphology in *Teucrium* L. (Labiatae). A taxonomic review. *An Jard Bot Madr* 57:277–297
- Nithaniyal S, Vassou SL, Poovitha S, Raju B, Parani M (2017) Identification of species adulteration in traded medicinal plant raw drugs using DNA barcoding. *Genome* 60:139–146
- Osman AK, Khalik KN, Osman AK, Boulos L (2012) Trichome micromorphology of egyptian *Ballota* (Lamiaceae) with emphasis on its systematic implication. *Pak J Bot* 44:33–46
- Paradis E, Schliep K (2019) ape 5.0: an environment for modern phylogenetics and evolutionary analyses in R. *Bioinformatics* 35:526–528. <https://doi.org/10.1093/bioinformatics/bty633>
- Patel M, Lee R, Merchant EV, Juliani HR, Simon J, Tepper BJ (2021) Descriptive aroma profiles of fresh sweet basil cultivars (*Ocimum spp.*): Relationship to volatile chemical composition. *J Food Sci* 86:3228–3239
- Paulus D, Valmorbidia R, Ramos CE (2019) Productivity and chemical composition of the essential oil of *Ocimum x citriodorum* Vis. according to ontogenetic and diurnal variation. *J Appl Res Med Aroma* 12:59–65
- Payne WW (1978) A glossary of plant hair terminology. *Brittonia* 30:239–255
- Pires TCSP, Dias MI, Barros L, Calhelha RC, Alves MJ, Oliveira MBPP, Santos-Buelga C, Ferreira ICFR (2018) Edible flowers as sources of phenolic compounds with bioactive potential. *Food Res Int* 105:580–588. <https://doi.org/10.1016/j.foodres.2017.11.014>
- Pospiech M, Javůrková Z, Hrabec P, Štarha P, Ljasovská S, Bednář J, Tremlová B (2021) Identification of pollen taxa by different microscopy techniques. *PLoS ONE* 16:e0256808. <https://doi.org/10.1371/journal.pone.0256808>
- Prinsi B, Morgutti S, Negrini N, Faoro F, Espen L (2019) Insight into composition of bioactive phenolic compounds in leaves and flowers of green and purple basil. *Plants* 9:22. <https://doi.org/10.3390/plants9010022>
- R Core Team (2022). R: A language and environment for statistical computing. R foundation for statistical computing, Vienna. <https://www.R-project.org>
- Raju AJS (1989) Reproductive ecology of *Ocimum americanum* L. and *O. basilicum* L. (Lamiaceae) in India. *Plant Species Biol* 4:107–116. <https://doi.org/10.1111/j.1442-1984.1989.tb00052.x>
- Rashid A, Anwar F, Qadir R, Sattar R, Tahir Akhtar M, Nisar B (2023) Characterization and biological activities of essential oil from flowers of sweet basil (*Ocimum basilicum* L.) selected from different regions of Pakistan. *J Essent Oil-Bear Plants* 26:95–107. <https://doi.org/10.1080/0972060X.2022.2155073>
- Rusydi A, Talip N, Latip J, Rahman RA, Sharif I (2013) Morphology of trichomes in *Pogostemon cablin* Benth. (Lamiaceae). *Aust J Crop Sci* 7:744–749
- Sanoj E, Deepa P (2021) Micromorphological variations of trichomes in the genus *Ocimum* L. *Plant Sci Today* 8(3):429–436
- Schliep KP (2011) phangorn: phylogenetic analysis in R. *Bioinformatics* 27:592–593. <https://doi.org/10.1093/bioinformatics/btq706>
- Sim LY, Abd Rani NZ, Husain K (2019) Lamiaceae: an insight on their anti-allergic potential and its mechanisms of action. *Front Pharmacol* 10:677. <https://doi.org/10.3389/fphar.2019.00677>
- Simon JE, Morales MR, Phippen WB, Fontes Vieira R, Hao Z (1999) Basil: a source of aroma compounds and a popular culinary and ornamental herb. In: Janick J (ed) *Perspectives on new crops and new uses*. ASHS Press, Alexandria, pp 499–505
- Smillie TJ, Khan IA (2010) A comprehensive approach to identifying and authenticating botanical products. *Clin Pharmacol* 87:175–186. <https://doi.org/10.1038/clpt.2009.287>
- Švecová E, Neugebauerova J (2010) A study of 34 cultivars of basil (*Ocimum* L.) and their morphological, economic and biochemical characteristics, using standardized descriptors. *Acta Univ Sapientiae: Alimentaria* 3:118–125
- Talamond P, Verdeil JL, Conéjéro G (2015) Secondary metabolite localization by Autofluorescence in living plant cells. *Molecules* 20:5024–5037. <https://doi.org/10.3390/molecules20035024>

- Thi Tran LT, Nguyen TK, Nguyen HT, Nguyen PP, Thi Dang NY, Tran MH, Tran Pham VP, Le AT (2022) Morpho-Anatomical Study And Botanical Identification of *Pogostemon auricularius* (L.) Hassk. (Lamiaceae). *Sci Prog* 105(2):003685042210941. <https://doi.org/10.1177/00368504221094156>
- Tian W, Liao Z, Zhang J (2017) An optimization of artificial neural network model for predicting chlorophyll dynamics. *Ecol Modell* 364:42–52
- Tungmunnithum D, Renouard S, Drouet S, Blondeau JP, Hano C (2020) A critical cross-species comparison of pollen from *Nelumbo nucifera* Gaertn vs. *Nymphaea lotus* L. for authentication of Thai medicinal herbal tea. *Plants* 9:921. <https://doi.org/10.3390/plants9070921>
- Uphof JCT (1962) Plant hairs. In: Zimmermann W, Ozenda PG (eds) *Encyclopedia of Plant Anatomy*, vol 5. Gebrüder Borntraeger, Berlin, pp 1–206
- Upton R, David B, Gafner S, Glasl S (2020) Botanical ingredient identification and quality assessment: strengths and limitations of analytical techniques. *Phytochem Rev* 19:1157–1177. <https://doi.org/10.1007/s11101-019-09625-z>
- Werker E (1993) Function of essential oil-secreting glandular hairs in aromatic plants of the Lamiaceae—a review. *Flavour Fragr J* 8:249–255
- Werker E, Ravid U, Putievsky E (1985a) Structure of glandular hairs and identification of the main components of their secreted material in some species of the Labiatae family. *Israel J Bot* 34:31–45
- Werker E, Ravid U, Putievsky E (1985b) Glandular hairs and their secretions in the vegetative and reproductive organs of *Salvia sclarea* and *S. dominica*. *Israel J Bot* 34:239–252
- Wesolowska A, Jadczyk D (2016) Composition of the essential oils from inflorescences, leaves and stems of *Ocimum basilicum* ‘cinnamon’ cultivated in North-western Poland. *J Essent Oil Bear Plants* 19:1037–1042
- Xiao S, Xu P, Deng Y, Dai X, Zhao L, Heider B et al (2021) Comparative analysis of chloroplast genomes of cultivars and wild species of sweetpotato (*Ipomoea batatas* [L.] Lam). *BMC Genom* 22:1–12
- Yao H, Song J, Liu C, Luo K, Han J, Li Y, Chen S (2010) Use of ITS2 region as the universal DNA barcode for plants and animals. *PLoS ONE* 5(10):e13102
- Zhang Y, Wang D, Li H et al (2023) Formation mechanism of glandular trichomes involved in the synthesis and storage of terpenoids in lavender. *BMC Plant Biol* 23:307. <https://doi.org/10.1186/s12870-023-04275-y>

Publisher's Note Springer Nature remains neutral with regard to jurisdictional claims in published maps and institutional affiliations.